

## **Elevated levels of 8-OHdG and PARK7/DJ-1 in peri-implantitis mucosa**

Gökhan Kasnak<sup>1,2</sup>, Erhan Fıratlı<sup>2</sup>, Eija Könönen<sup>1</sup>, Vakur Olgac<sup>3</sup>, Fares Zeidán-Chuliá<sup>1</sup>, Ulvi Kahraman GURSOY<sup>1</sup>

1 Institute of Dentistry, University of Turku, Turku, Finland

2 Faculty of Dentistry, Istanbul University, Istanbul, Turkey

3 Institute of Oncology, Department of Tumor Pathology, Istanbul University, Istanbul, Turkey

### **Corresponding author:**

Gökhan Kasnak (DDS, PhD)

Department of Periodontology, Institute of Dentistry, University of Turku

Lemminkäisenkatu 2, 20520 Turku, Finland

Email: [kasnak@istanbul.edu.tr](mailto:kasnak@istanbul.edu.tr); [gokhan.kasnak@utu.fi](mailto:gokhan.kasnak@utu.fi)

## **Abstract**

**Background:** Reactive oxygen species contribute to periodontal tissue homeostasis under control of anti-oxidative responses. Disruption in this balance induces severe inflammation and extended tissue degradation.

**Purpose:** Aim of this study was to identify the expression levels of nuclear factor, erythroid 2 like 2 (NFE2L2/NRF2), Parkinsonism associated deglycase (PARK7/DJ-1), kelch-like ECH associated protein 1 (KEAP1), and 8-hydroxy-deoxyguanosine (8-OHdG) in peri-implant mucosal tissues affected by peri-implantitis, and to compare the levels to those of periodontally diseased and healthy tissue samples.

**Methods:** Tissue biopsies were collected from systemically healthy, non-smoking 12 periimplantitis patients, 13 periodontitis patients, and 13 periodontally healthy controls. Expression levels of NFE2L2/NRF2, PARK7/DJ-1, KEAP1, and 8-OHdG in tissue samples were analyzed immunohistochemically. Statistical analysis was performed by one-way ANOVA with Tukey's HSD test.

**Results:** Inflammatory cell infiltration in the connective tissue and loss of architecture in the spinous layer of the epithelium were prominent in peri-implantitis. Proportions of 8-OHdG and PARK7/DJ-1 expressing cells were elevated in both peri-implantitis (P 5 .025 for 8-OHdG and P 5 .014 for PARK7/DJ-1) and periodontitis (P 5 .038 for 8-OHdG and P 5 .012 for PARK7/DJ-1) groups in comparison with controls. Staining intensities of 8-OHdG and PARK7/DJ-1 were higher in the periodontitis and peri-implantitis groups than in the control (P < .01) groups. There was no difference in the expression levels of NFE2L2/NRF2 between the groups. KEAP1 was not observed in any tissue sample.

**Conclusions:** Peri-implantitis is characterized by severe inflammation and architectural changes in the epithelium and connective tissue. The expressions of 8-OHdG and PARK7/DJ-1 are elevated in both peri-implantitis and periodontitis.

## **Keywords**

oxidative stress, peri-implant lesion, periodontitis

## Introduction

Reactive oxygen species (ROS) take part in cell signaling, proliferation, and renewal that are crucial for the host tissue metabolism.<sup>1</sup> During infectious processes, an excessive accumulation of ROS leads to oxidative stress, which is responsible for the damage of lipids, carbohydrates, proteins, and deoxyribonucleic acid (DNA). 8-Hydroxydeoxyguanosine (8-OHdG) is a prominent marker of DNA damage, and its increased levels in body fluids can act as an indicator of excessive oxidative stress.<sup>2</sup> Main mediators of the cytoprotective pathway against oxidative stress are Parkinsonism associated deglycase (PARK7/DJ-1), nuclear factor, erythroid 2 like 2 (NFE2L2/NRF2), and kelch-like ECH associated protein 1 (KEAP1).<sup>3</sup> NFE2L2/NRF2, the major regulator of the antioxidative response mechanism, is retained in the cytoplasm by KEAP1 in basal conditions, and its stabilization and transcriptional functions are determined by PARK7/DJ-1.<sup>4</sup> When the levels of ROS elevate, NFE2L2/NRF2 detaches from its binder KEAP1 and translocates to the nucleus to activate the genes for the expression of antioxidative response elements (eg, catalase, superoxide dismutase, NAD(P)H:quinone oxidoreductase, and glutathione peroxidase).<sup>5</sup> PARK7/DJ-1 controls the turnover of NFE2L2/NRF2.<sup>6</sup> The impact of the PARK7/DJ-1, NFE2L2/NRF2, and KEAP1 cascade in chronic diseases, especially in atherosclerosis and neurodegenerative diseases, has been well demonstrated.<sup>7,8</sup>

Peri-implantitis and periodontitis are characterized by soft tissue inflammation and bone destruction, however, in peri-implantitis neutrophil and macrophage infiltration and extension of tissue destruction are more prominent than in periodontitis.<sup>9</sup> Excessive oxidative stress seems to play an important role in the destruction of periodontal tissues.<sup>10</sup> Elevated levels of 8-OHdG in gingival crevicular fluid and saliva are suggested as a prominent marker of periodontal tissue break down,<sup>11</sup> and decreased gingival crevicular fluid 8-OHdG levels have been associated with the successful periodontal treatment of chronic periodontitis.<sup>12</sup> The cytoprotective role of KEAP1 and NFE2L2/NRF2 in the reduction of inflammatory signaling and oxidative damage is highly important and has been reviewed recently.<sup>13</sup> Previous studies have indicated that NFE2L2/NRF2 activation suppresses osteoclastogenesis,<sup>14</sup> it protects periodontal ligament stem cells from oxidative stress-related apoptosis,<sup>15</sup> and its down-regulation in oral neutrophils is associated with chronic periodontitis in humans.<sup>16</sup> Oxidative stress and antioxidative response biomarkers have been reported from salivary and gingival crevicular fluid samples of periodontitis and peri-

implantitis patients,<sup>17</sup> however, up to our knowledge, the PARK7/DJ-1, NFE2L2/NRF2, and KEAP1 cascade has not been investigated in peri-implantitis tissues before. The excessive accumulation of ROS is critical in the initiation and progression of periodontal diseases, therefore, we hypothesized that a deficiency in its regulators has a role in the pathogenesis of periodontitis and peri-implantitis. The aim was to determine the expression levels of 8-OHdG, NFE2L2/NRF2, PARK7/DJ-1, and KEAP1 in peri-implant soft tissue and further, to compare them with levels in gingival samples collected from periodontitis patients and periodontally healthy controls.

## **Methods**

### **Study population**

Patients with peri-implantitis (seven males and five females with age range of 36–59 years) or with periodontitis (six males and seven females with age range of 29–54 years), referred to the University of Istanbul Faculty of Dentistry Department of Periodontology were recruited for the study. They were systemically healthy and never smoked. Thirteen periodontally healthy individuals (eight males and five females with age range of 28–55 years) served as their controls. Exclusion criteria were: active caries lesions, oral mucosal diseases, ongoing orthodontic therapy, pregnancy, lactation, and use of prescribed or non-prescribed drugs and antibiotics prior to recruitment. All implants had been in function at least three years without any sign of mobility (bone level, internal hex type abutment connection). The Ethics Committee of the University of Istanbul, Faculty of Dentistry, approved the study protocol according to the Helsinki Declaration (2017/41).

A single calibrated examiner (G.K.) carried out periodontal examinations, including plaque index (PI),<sup>18</sup> gingival index (GI),<sup>19</sup> clinical attachment level (CAL), bleeding on probing (BOP),<sup>20</sup> and probing pocket depth (PPD) measurements at four sites of all teeth and dental implants by using a periodontal probe (UNC-15, Hu-Friedy, Chicago, IL, USA), and alveolar bone loss measurements from orthopantomographs. Orthopantomographs were taken from all individuals using an extra oral imaging system (KODAK 9000 3D, Carestream Dental LLC, Atlanta, GA, USA) and evaluated with a specialized computer software (Dental Imaging Software CS 3D, Carestream Dental LLC, Atlanta, GA, USA), which is designed specifically for storage and interpretation of the digital data received

from the X-ray machine. For the control and periodontitis groups, the distance between the cemento-enamel junction and the most coronal part of the bone defect on both mesial and distal sites were measured, and the ratio to the length of the root calculated to determine the bone loss. For the evaluation of bone loss around implants, the shoulder of the implants was selected as a reference point, and the distance from this point to the marginal bone level was measured in millimeters on both mesial and distal sites.

All study participants had at least 15 teeth. Individuals who had three or more teeth with CAL  $\geq 5$  mm and PPD  $\geq 5$  mm in at least two separate quadrants with the presence of BOP and radiographic alveolar bone loss at least 25% of the root length were diagnosed as having moderate to severe periodontitis.<sup>21</sup> Individuals who had CAL  $\geq 5$  mm and PPD  $\geq 5$  mm on both the mesial and distal site of dental implants accompanied with BOP either with or without suppuration/exudate, and  $\geq 3$  mm radiographic bone loss were recruited as peri-implantitis patients.<sup>22,23</sup> Periodontitis was not observed in peri-implantitis patients. Individuals having no sites with PPD  $> 3$  mm and CAL  $> 2$  mm were identified as periodontally healthy.<sup>23</sup>

### **Tissue samples**

Gingival biopsies were taken from deepened pockets of the peri-implantitis and periodontitis patients during their surgical treatments and from the periodontally healthy controls during their crown lengthening procedures. Gingival biopsy sites of the controls did not have any sign of inflammation or radiographic alveolar bone loss. In order to obtain the bottom of the periodontal pocket and sulcular epithelium, internal beveled incisions were performed. After obtaining gingival and peri-implant mucosal biopsies, the oral epithelium was stained by a tissue marking dye (CDI's<sup>®</sup> tissue marking dye, 0724-2, Cancer Diagnostics Inc., Dunham, NC, USA) to distinguish the oral and sulcular epithelium accurately during the microscopic evaluation. All tissue specimens were fixed in 4% formalin for less than 24 h and embedded in paraffin blocks, and immunohistochemical evaluations were performed at the University of Turku, Institute of Dentistry laboratories.

### **Immunohistochemical stainings**

Tissue samples in paraffin blocks were cut into 5  $\mu\text{m}$  thick sections and placed onto slides

for immunohistochemistry procedures. The sections were deparaffinized and immunostained for 8-OHdG (SC 393870, Santa Cruz Biotechnology, Dallas, TX, USA), PARK7/DJ-1 (SC 32874, Santa Cruz Biotechnology, Dallas, TX, USA), NFE2L2/NRF2 (SC 722, Santa Cruz Biotechnology, Dallas, TX, USA), and KEAP1 (SC 33569, Santa Cruz Biotechnology, Dallas, TX, USA). Immunohistochemical stainings were carried out for all markers using the routine procedures with an automated immunostainer (TechMate, DAKO, Glostrup, Denmark). Briefly, antigen retrieval in a microwave twice for 5 min in 1 mmol/L citrate buffer (pH 6.0) was followed by endogenous peroxidase blocking by 3% H<sub>2</sub>O<sub>2</sub>. The primary antibody was detected by a biotinylated secondary antibody (Dako REAL™ Detection System, K5001, Dako, Glostrup, Denmark), coupled with streptavidin-horseradish peroxidase, and visualized with 3,3'-diaminobenzidine tetrahydrochloride in HRP buffer (Dako REAL™ Detection System, K5001, Dako, Glostrup, Denmark).

The validity of immunohistochemical stainings was tested in bronchial alveolar tissue for 8-OHdG, in testis tissue for PARK7/DJ-1, and in kidney tissue for NFE2L2/NRF2 and KEAP1. As negative controls, immunohistochemical stainings without primary antibodies were performed.

Tissue specimens were preliminarily evaluated under a light microscope (Leica DMLB, Leica, Wetzlar, Germany) to define the region of interest (ROI), which was the most apical part of the sulcus epithelium with morphological integrity that allows cell counting. These ROIs were imaged under 20X to 100X magnification, and the high-resolution images (2088 x 1550 pixels; 0.251 mm<sup>2</sup>) were captured for the assessment of the stainings (Leica DC 300 V 2.0 Leica, Wetzlar, Germany). To determine the proportions of positively stained epithelial cells, the tissue specimens were classified into three staining groups according to the intensity of their staining levels of 8-OHdG, PARK7/DJ-1, NFE2L2/NRF2, and KEAP1. Cells without any sign of staining were grouped as non-stained (2), cells with either cytoplasm or nucleus staining in a partial manner were grouped as weakly stained (1), and cells with partial staining in both cytoplasm and nucleus or full cytoplasm staining were grouped as strongly stained (11).<sup>24</sup> Cell counting was performed manually. In addition to the cell counting analyses, the captured images were evaluated by the ImageJ software (version 1.46c; Rasband WS, National Institutes of Health, Bethesda, MD, USA) with immunohistochemistry image analysis toolbox plugin version 2 (National Institutes of

Health, Bethesda, MD, USA) to confirm the staining intensity of all tissue specimens. Intensities of the staining were determined from both epithelium and connective tissue.

### **Statistical analysis**

The comparison of the staining levels of 8-OHdG, PARK7/DJ-1, NFE2L2/NRF2, and KEAP1 within and between the sample groups were carried out by one-way ANOVA with Tukey's HSD test. A  $p < .05$  value was considered as significant. All tests were performed with a statistical software (SPSS v.24, IBM, Chicago, IL, USA).

### **Results**

#### **Demographic data and clinical parameters**

The demographic data and clinical parameters are given in Table 1. All clinical parameters were higher in the peri-implantitis ( $p < .001$ ) and periodontitis ( $p < .001$ ) groups in comparison to those of periodontally healthy controls. There was no statistically significant difference in terms of age and gender ( $p > .05$ ) between the groups.

#### **Tissue morphology and architecture**

There was an extensive inflammatory cell infiltration and accumulation in lamina propria of peri-implantitis tissue samples in comparison to that of the periodontitis group. Moreover, a disrupted epithelial architecture and loss of spinous layer thickness was seen in peri-implantitis samples, but not in the periodontitis group.

#### **Expression of 8-OHdG, PARK7/DJ-1, NFE2L2/NRF2, and KEAP1**

In the epithelium, 8-OHdG and PARK7/DJ-1 stained cells were mainly located at the basal layer in samples taken from periodontally healthy controls but at all layers in periodontitis and peri-implantitis samples (Figures 1A-F and 2A-F), whereas NFE2L2/NRF2 stained cells were widely spread at epithelial layers in both diseased and healthy tissue samples (Figure 3A-F). In the connective tissue of all samples, there was a

significant number of 8-OHdG and PARK7/DJ-1 stained cells, while the number of NFE2L2/NRF2 stained cells was low. KEAP1 stained cells were not observed in any tissue sample (Supporting Information Figure S1A-F). The validity of the stainings was tested on human tissues as suggested by the producer company of the primary antibodies used, and the tissues stained positively (Supporting Information Figure S2).

The proportion of 8-OHdG expressing cells in the epithelium of peri-implantitis (p 5 .025) and periodontitis (p 5.038) samples was significantly higher than in controls. Also, the number of PARK7/DJ-1 expressing epithelial cells was elevated in peri-implantitis (p 5.014) and periodontitis (p 5.012) tissue samples compared with periodontally healthy samples. There was no difference in the number of NFE2L2/NRF2 expressing epithelial cells between the study groups (for peri-implantitis p 5.827 and for periodontitis p 5 .893). Correspondingly intensities (performed via ImageJ software) of the 8-OHdG and PARK7/DJ-1 stainings were stronger in the periodontitis and peri-implantitis groups than in control (p < .01). No difference was observed in staining intensity of NFE2L2/NRF2 (for peri-implantitis p 5.056 and for periodontitis p 5.085) (Figure 4A-D).

## **Discussion**

The impact of elevated 8-OHdG levels on periodontal destruction has been previously demonstrated, however, our study is the first one where the expression levels of 8-OHdG, PARK7/DJ-1, NFE2L2/NRF2, and KEAP1 have been investigated in tissue samples collected from peri-implantitis lesions. Increased 8-OHdG and PARK7/DJ-1 levels were found in the epithelium and connective tissue of peri-implantitis and periodontitis samples, while expression levels of NFE2L2/NRF2 did not show any alterations between the groups.

A unique finding in peri-implantitis tissue samples was the disrupted architecture of epithelium, which was defined by the loss of spinous layer thickness. Additionally, an increased inflammatory cell infiltration and loss of collagen structure was seen in the peri-implantitis group in comparison with the periodontitis group. In animal models, it has been demonstrated that during the early phase of inflammation, both gingiva and peri-implant mucosa show an increase in numbers of inflammatory cells and a loss of collagen but peri-

implantitis lesions were larger and extended closer to the bone crest than periodontitis lesions.<sup>25,26</sup> In human biopsies, neutrophilic granulocytes and macrophages have been showed to occur in higher proportions and the extension of tissue destruction to be more obvious in peri-implantitis when compared with periodontitis.<sup>27,28</sup>

Smoking has been substantiated as a risk factor for periodontal tissue degradation<sup>29</sup> and the effect of smoking on oxidative stress levels has been shown in chronic periodontitis.<sup>11</sup> One limitation of our study is that the study population did not include smokers. Thus, expression of 8-OHdG, PARK7/DJ-1, NFE2L2/NRF2, and KEAP1 in smokers with peri-implantitis, periodontitis, and periodontally healthy individuals need to be evaluated in further studies. In the present study, control tissue samples were obtained during crown lengthening procedures of periodontally healthy individuals without signs of clinical inflammation (no bleeding on probing) in sampling sites, however, subclinical inflammation was observed in a few samples. The history of the periodontal status and previous treatment information of the peri-implantitis patients were not available to us. Therefore, in the absence of previous radiographic recordings, we followed the guidelines of the consensus report,<sup>22</sup> and a threshold of 3 mm was applied to define peri-implantitis related bone loss. Orthopantomographs provide a good overview on the marginal bone level at a little radiation dose, however, due to the mandibular angle and the width of the jaws of individuals, inconsistent magnification and geometric distortions might occur.<sup>30</sup> The trustworthiness of the measurements should be secured by positioning the objects in focal trough zone. Healthy peri-implant mucosa samples were not collected due to ethical reasons. Finally, as there are no previous studies available on 8-OHdG, NFE2L2/NRF2, and PARK7/ DJ-1 levels in oral tissues, the study size was defined according to studies, where immunohistochemical methods were used to determine the tissue levels of immune response proteins in gingival biopsies collected from individuals with periodontitis.<sup>24,31</sup>

The measurement of 8-OHdG levels is considered a reliable technique for the detection of elevated oxidative stress, and increased 8-OHdG levels have been demonstrated in mouse and human periodontitis tissue samples.<sup>32</sup> Elevated levels of 8-OHdG were related to clinically measurable residual inflammation after treatment of periodontitis.<sup>33</sup> In the present study, we observed an enhanced number of 8-OHdG stained cells in the peri-implantitis and periodontitis tissue samples. Interestingly, in control samples, 8-OHdG was observed mainly

at the basal layer of the epithelium, while in the peri-implantitis group it was at all layers of the epithelium and also in connective tissue. Physiological levels of ROS influence the cellular proliferation and differentiation of cells in a variety of biological systems.<sup>34</sup> 8-OHdG expression at the basal layers of the epithelium in control tissues of our study may be related to metabolically active, proliferating keratinocytes regulated by the endogenously-produced and well-controlled ROS levels.<sup>35</sup> On the other hand, elevated levels of 8-OHdG at all epithelial layers and in lamina propria in the tissues affected by peri-implantitis may be due to the presence of exogenous and highly destructive ROS, which are mainly produced by inflammatory cells, such as neutrophils and macrophages. To the best of our knowledge, there are no data on 8-OHdG levels in tissues affected by peri-implantitis, therefore we could not compare our results with the literature.

PARK7/DJ-1 was identified in the healthy gingiva,<sup>36</sup> however, data on its role in peri-implant and periodontal diseases are unavailable. It has been demonstrated that PARK7/DJ-1 attenuates the expression of pro-inflammatory mediators in microglia and astrocytes.<sup>37</sup> In the present study, PARK7/DJ-1 was observed at the basal layer of the control samples, whereas it was found at elevated levels at all layers of the epithelium and connective tissue in peri-implantitis and periodontitis samples. Indeed, these findings fit well with the localization and expression of 8-OHdG in peri-implantitis and periodontitis. Expression of PARK7/DJ-1 is dependent on ROS; an increase in endogenous ROS, for example, by bacterial endotoxins, activates overexpression of PARK7/DJ-1 in tissues.<sup>38,39</sup> Dendritic cells generate ROS during antigen presentation<sup>40</sup> and T-cell interactions and toll-like receptor ligation can improve a weak ROS generation in dendritic cells.<sup>41</sup> The present results indicate that 8-OHdG and PARK7/DJ-1 activation at basal layers of the epithelium is normal in healthy tissues, while their levels increase significantly during inflammation in tooth- and implant-surrounding tissues.

In the present study, the number of NFE2L2/NRF2 stained epithelial cells in peri-implantitis, periodontitis, and control samples was similar. Also, the majority of NFE2L2/NRF2 positive cells was localized at the epithelium, while only a limited number of NFE2L2/NRF2 positive cells was seen in the connective tissue. NFE2L2/NRF2 translocation into the nucleus is considered an essential step in its activation, however, there was no evidence on this translocation in our study, whereas cytoplasmic NFE2L2/NRF2 was evident in both peri-

implantitis and periodontitis tissue samples. Osteoclastic bone resorption has been linked to NFE2L2/NRF2 deficiency<sup>42</sup> and attenuated osteoclastogenesis has been observed via activation of NFE2L2/NRF2 in a mouse model.<sup>14</sup> Moreover, attachment loss and alveolar bone destruction have been demonstrated in relation to elevated 8-OHdG levels in NFE2L2/NRF2 knocked out mice with chronic periodontitis, and this finding was linked to the down-regulation of the NFE2L2/NRF2 pathway through the increase of oral neutrophils.<sup>16</sup> Furthermore, it was recently suggested that activation of the NFE2L2/NRF2 pathway, related to its role in the transcription of anti-oxidative enzymes, can be used as an adjuvant therapy in the treatment of periodontitis.<sup>13</sup> In the present study peri-implantitis and periodontitis groups, NFE2L2/NRF2 levels did not alter against elevated levels of 8-OHdG. On the one hand, suppression or insufficient expression of NFE2L2/NRF2 may be a reason for its unaltered levels and have role in the disease progression. On the other hand, although NFE2L2/NRF2 is the major mediator of antioxidative response, other proteins, like O class of the forkhead box (FOXOs), are also responsible for the transcription of antioxidants.<sup>43</sup> The activation of FOXO1 transcription by *Porphyrromonas gingivalis*, a major periodontal pathogen, has been demonstrated in gingival epithelial cells.<sup>44</sup> Further studies are warranted to clarify the impact of FOXOs and related antioxidants in the progression of periodontal and peri-implant diseases.

The protective role of NFE2L2/NRF2 against periodontitis has been demonstrated in a KEAP1-dependent oxidative stress detector- luciferase mouse model.<sup>45</sup> Also, the association of KEAP1-NFE2L2/ NRF2 and oral cell carcinoma has been shown immunohistochemically.<sup>46</sup> In our study, no KEAP1 was observed in any of the tissue samples. An explanation could be that KEAP1 remains under the detection level of the methodology used, however, when tested for validity in kidney tissue, the same protocol demonstrated KEAP1 positive cells. Therefore, in the limits of this study, the absence of KEAP1 in gingival and peri-implant tissues was unexplained.

In conclusion, 8-OHdG and PARK7/DJ-1 are expressed at basal layers of the epithelium in healthy gingiva, while their levels increase significantly in the epithelium and connective tissue during periodontitis and peri-implantitis. In diseased peri-implant tissues, an increased inflammatory cell infiltration and a disrupted epithelial cell architecture are observed in peri-implantitis.

## References

1. Muniz FW, Nogueira SB, Mendes FL, et al. The impact of antioxidant agents complimentary to periodontal therapy on oxidative stress and periodontal outcomes: a systematic review. *Arch Oral Biol.* 2015;60(9):1203–1214.
2. Di Minno A, Turnu L, Porro B, et al. 8-hydroxy-2-deoxyguanosine levels and cardiovascular disease: a systematic review and meta- analysis of the literature. *Antioxid Redox Signal.* 2016;24(10):548– 555.
3. Sun Q, Shen ZY, Meng QT, Liu HZ, Duan WN, Xia ZY. The role of DJ-1/Nrf2 pathway in the pathogenesis of diabetic nephropathy in rats. *Ren Fail.* 2016;38(2):294–304.
4. Yan YF, Yang WJ, Xu Q, et al. DJ-1 upregulates anti-oxidant enzymes and attenuates hypoxia/re-oxygenation-induced oxidative stress by activation of the nuclear factor erythroid 2-like 2 signaling pathway. *Mol Med Rep.* 2015;12(3):4734–4742.
5. Kansanen E, Kuosmanen SM, Leinonen H, Levonen AL. The Keap1- Nrf2 pathway: mechanisms of activation and dysregulation in can- cer. *Redox Biol.* 2013;1(1):45–49.
6. Milani P, Ambrosi G, Gammoh O, Blandini F, Cereda C. SOD1 and DJ-1 converge at Nrf2 pathway: a clue for antioxidant therapeutic potential in neurodegeneration. *Oxid Med Cell Longev.* 2013;2013: 836760.
7. Johnson DA, Johnson JA. Nrf2—a therapeutic target for the treat- ment of neurodegenerative diseases. *Free Radic Biol Med.* 2015;88 (Pt B):253–267.
8. Mimura J, Itoh K. Role of Nrf2 in the pathogenesis of atherosclerosis. *Free Radic Biol Med.* 2015;88(Pt B):221–232.
9. Berglundh T, Zitzmann N, Donati M. Are peri-implantitis lesions different from periodontitis lesions?. *J Clin Periodontol.* 2011;38: 188–202.
10. Kanzaki H, Shinohara F, Itohiya K, et al. RANKL induces Bach1 nuclear import and attenuates Nrf2-mediated antioxidant enzymes, thereby augmenting intracellular reactive oxygen species signaling and osteoclastogenesis in mice. *Faseb J.* 2017;31(2):781–792.
11. Hendek MK, Erdemir EO, Kisa U, Ozcan G. Effect of initial peri- odontal therapy on oxidative stress markers in gingival crevicular fluid, saliva, and serum in smokers and non-smokers with chronic periodontitis. *J Periodontol.* 2015;86(2):273–282.
12. Dede FÖ Ozden FO, Avcı B. 8-hydroxy-deoxyguanosine levels in gingi- val crevicular fluid and saliva in patients with chronic periodontitis after initial periodontal treatment. *J*

- Periodontol.* 2013;84(6):821–828.
13. Chiu AV, Saigh MA, McCulloch CA, Glogauer M. The role of Nrf2 in the regulation of periodontal health and disease. *J Dent Res.* 2017; 96(9):975–983.
  14. Kanzaki H, Shinohara F, Kajiya M, Fukaya S, Miyamoto Y, Nakamura Y. Nuclear Nrf2 induction by protein transduction attenuates osteoclastogenesis. *Free Radic Biol Med.* 2014;77:239–248.
  15. Liu Y, Yang H, Wen Y, et al. Nrf2 inhibits periodontal ligament stem cell apoptosis under excessive oxidative stress. *Int J Mol Sci.* 2017; 18:1076–1092.
  16. Sima C, Aboodi GM, Lakschevitz FS, Sun C, Goldberg MB, Glogauer M. Nuclear factor erythroid 2-related factor 2 down-regulation in oral neutrophils is associated with periodontal oxidative damage and severe chronic periodontitis. *Am J Pathol.* 2016;186(6):1417–1426.
  17. Sánchez-Siles M, Lucas-Azorin J, Salazar-Sánchez N, Carbonell-Meseguer L, Camacho-Alonso F. Salivary concentration of oxidative stress biomarkers in a group of patients with peri-implantitis: a transversal study. *Clin Implant Dent Relat Res.* 2016;18(5):1015–1022.
  18. Silness J, Loe H. Periodontal disease in pregnancy. II. Correlation between oral hygiene and periodontal condition. *Acta Odontol Scand.* 1964;22:121–135.
  19. Loe H, Silness J. Periodontal disease in pregnancy. I. Prevalence and severity. *Acta Odontol Scand.* 1963;21:533–551.
  20. Ainamo J, Bay I. Problems and proposals for recording gingivitis and plaque. *Int Dent J.* 1975;25(4):229–235.
  21. American academy of periodontology task force report on the update to the 1999 classification of periodontal diseases and conditions. *J Periodontol.* 2015;86(7):835–838.
  22. Sanz M, Chapple IL. Clinical research on peri-implant diseases: consensus report of working group 4. *J Clin Periodontol.* 2012;39: 202–206.
  23. Freira SD, Silva GLM, Cortelli JR, Costa JE, Cots FO. Prevalence and risk variables for peri-implant disease in Brazilian subjects. *J Clin Periodontol.* 2006;33:929–935.
  24. Yılmaz D, Güncü GN, Könenen E, Barış E, Çağlayan F, Gursoy UK. Overexpressions of hBD-2, hBD-3, and hCAP18/LL-37 in gingiva of diabetics with periodontitis. *Immunobiology.* 2015;220(11):1219–1226.
  25. Heitz-Mayfield LJ, Lang P. Comparative biology of chronic and aggressive periodontitis vs. peri-implantitis. *Periodontol 2000.* 2010; 53(1):167–181.

26. Carcuac O, Albouy JP, Abrahamsson I, Linder E, Larsson L, Berglundh T. Experimental periodontitis and peri-implantitis in dogs. *Clin Oral Implants Res.* 2013;24(4):363–371.
27. Carcuac O, Berglundh T. Composition of human peri-implantitis and periodontitis lesions. *J Dent Res.* 2014;93(11):1083–1088.
28. Lang NP, Berglundh T. Peri-implant disease: where are we now? Consensus of the seventh European workshop on periodontology. *J Clin Periodontol.* 2011;38:178–181.
29. Johannsen A, Susin C, Gustafsson A. Smoking and inflammation: evidence for a synergistic role in chronic disease. *Periodontol 2000.* 2014;64(1):111–126.
30. Riecke B, Friedrich RE, Schulze D, et al. Impact of malpositioning on panoramic radiography in implant dentistry. *Clin Oral Invest.* 2015; 19(4):781–790.
31. Lapérine O, Cloitre A, Caillon J, et al. Interleukin-33 and RANK-L interplay in the alveolar bone loss associated to periodontitis. *PLoS One.* 2016;11(12):e0168080.
32. Cheng R, Choudhury D, Liu C, Billet S, Hu T, Bhowmick NA. Gingival fibroblasts resist apoptosis in response to oxidative stress in a model of periodontal diseases. *Cell Death Discov.* 2015;1(1):15046.
33. Kurgan Ş, Önder C, Altınöz SM, et al. High sensitivity detection of salivary 8-hydroxy deoxyguanosine levels in patients with chronic periodontitis. *J Periodontal Res.* 2015;50(6):766–774.
34. Jones RM, Luo L, Ardita CS, et al. Symbiotic lactobacilli stimulate gut epithelial proliferation via Nox-mediated generation of reactive oxygen species. *Embo J.* 2013;32(23):3017–3028.
35. Gao X, Xing D. Molecular mechanisms of cell proliferation induced by low laser irradiation. *J Biomed Sci.* 2009;16(1):4.
36. Yaprak E, Kasap M, Akpınar G, et al. The prominent proteins expressed in healthy gingiva: a pilot exploratory tissue proteomics study. *Odontology.* 2017;106:19–28.
37. Kim JH, Choi DJ, Jeong HK, et al. DJ-1 facilitates the interaction between STAT1 and its phosphatase, SHP-1, in brain microglia and astrocytes: a novel anti-inflammatory function of DJ-1. *Neurobiol Dis.* 2013;60:1–10.
38. Chan JY, Chan SH. Activation of endogenous antioxidants as a common therapeutic strategy against cancer, neurodegeneration and cardiovascular diseases: a lesson learnt from DJ-1. *Pharmacol Ther.* 2015;156:69–74.
39. Shen Z-Y, Sun Q, Xia Z-Y, et al. Overexpression of DJ-1 reduces oxidative stress and

- attenuates hypoxia/reoxygenation injury in NRK-52E cells exposed to high glucose. *Int J Mol Med*. 2016;38(3): 729–736.
40. Matsue H, Edelbaum D, Shalhevet D, et al. Generation and function of reactive oxygen species in dendritic cells during antigen presentation. *J Immunol*. 2003;171(6):3010–3018.
41. El-Awady A, Arce RM, Cutler CW. Dendritic cells: microbial clearance via autophagy and potential immunobiological consequences for periodontal disease. *Periodontol 2000*. 2015;69(1):160–180.
42. Hyeon S, Lee H, Yang Y, Jeong W. Nrf2 deficiency induces oxidative stress and promotes RANKL-induced osteoclast differentiation. *Free Radic Biol Med*. 2013;65:789–799.
43. Wang Y, Zhou Y, Graves DT. FOXO transcription factors: their clinical significance and regulation. *Biomed Res Int*. 2014;2014:1.
44. Wang Q, Sztukowska M, Ojo A, Scott DA, Wang H, Lamont RJ. FOXO responses to *Porphyromonas gingivalis* in epithelial cells. *Cell Microbiol*. 2015;17(11):1605–1617.
45. Kataoka K, Ekuni D, Tomofuji T, et al. Visualization of oxidative stress induced by experimental periodontitis in Keap1-dependent oxidative stress detector-luciferase mice. *Int J Mol Sci*. 2016;17(11):1907.
46. Huang CF, Zhang L, Ma SR, et al. Clinical significance of Keap1 and Nrf2 in oral squamous cell carcinoma. *PLoS One*. 2013;8(12): e83479.

## Figures

Figure.1

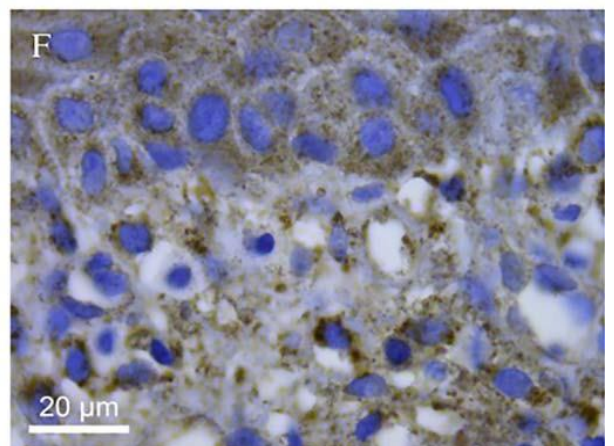
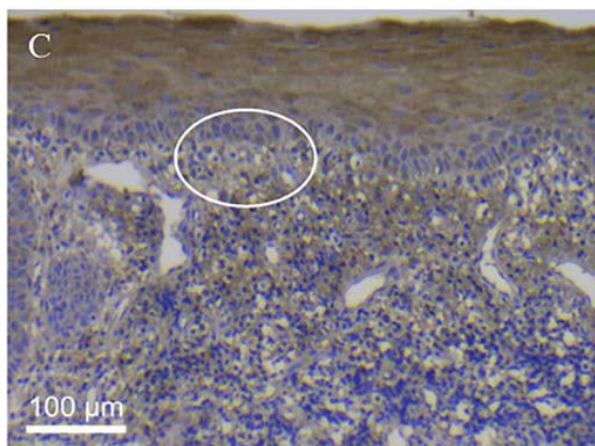
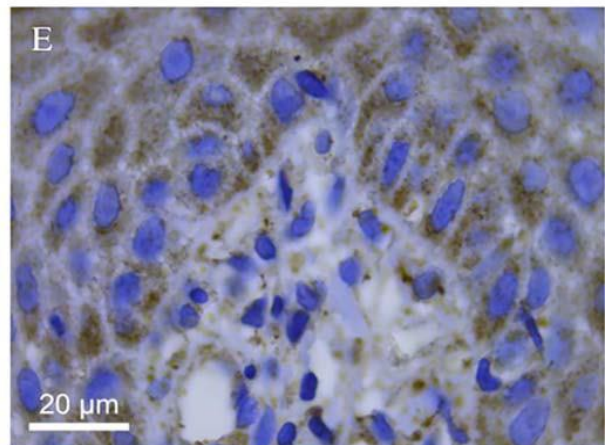
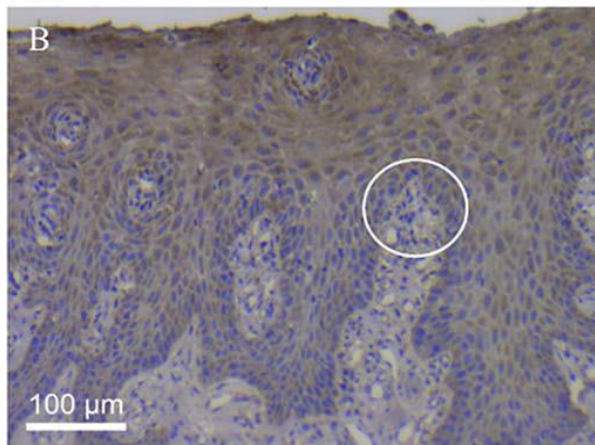
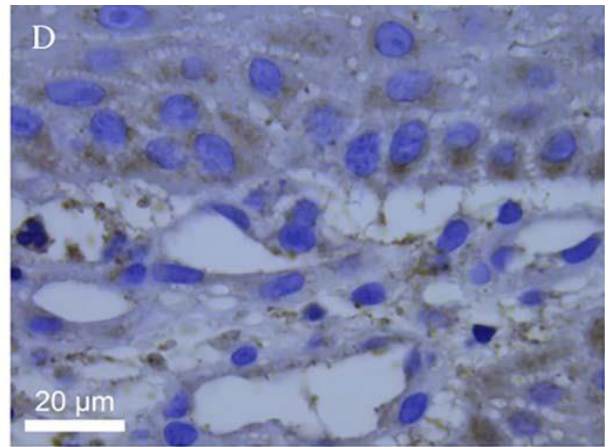
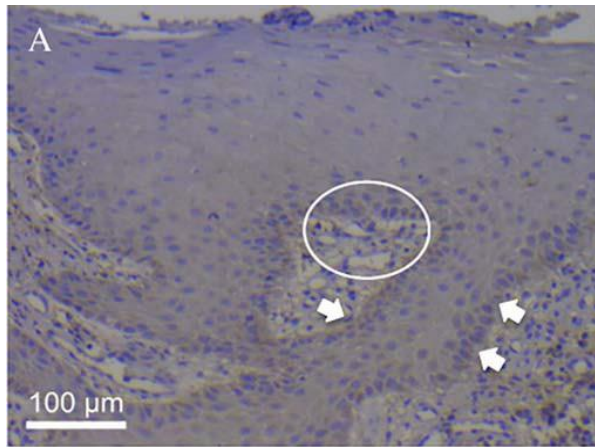
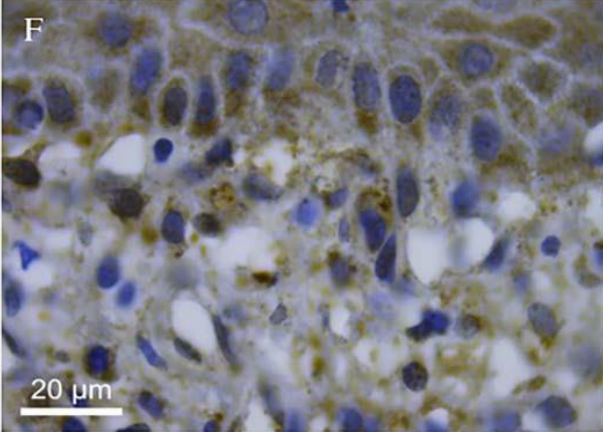
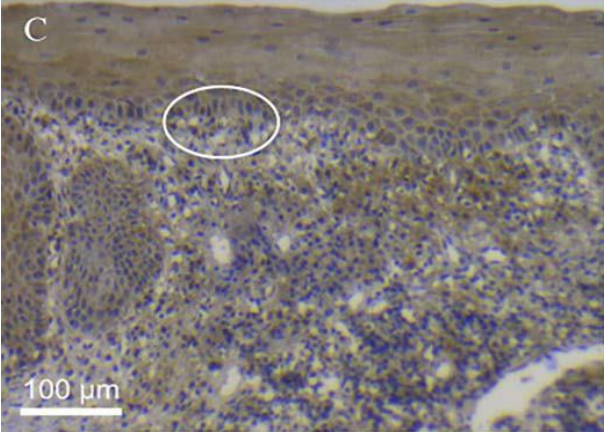
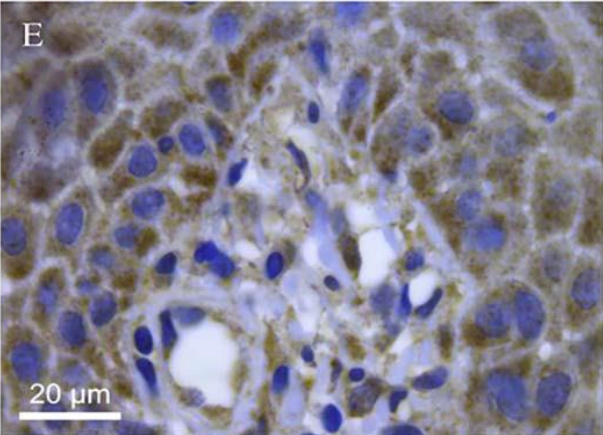
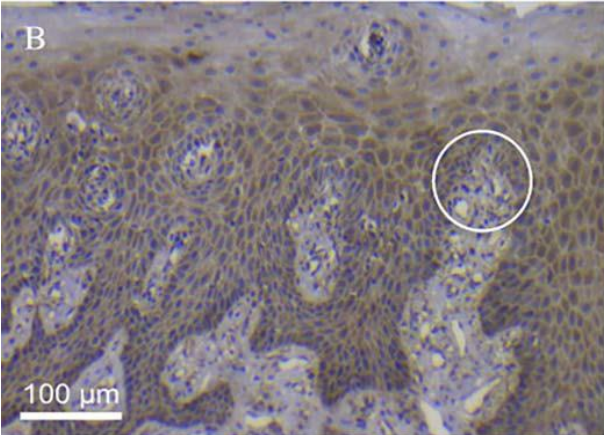
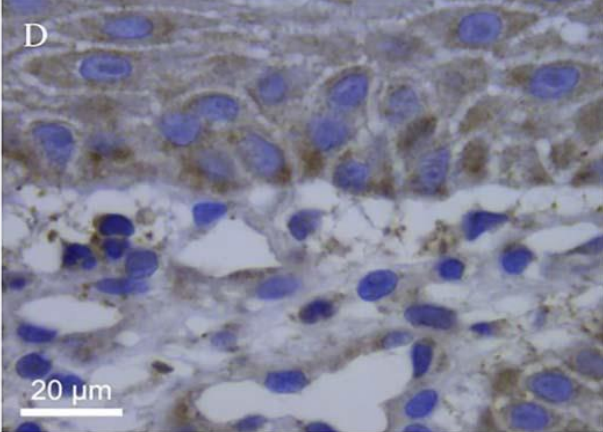
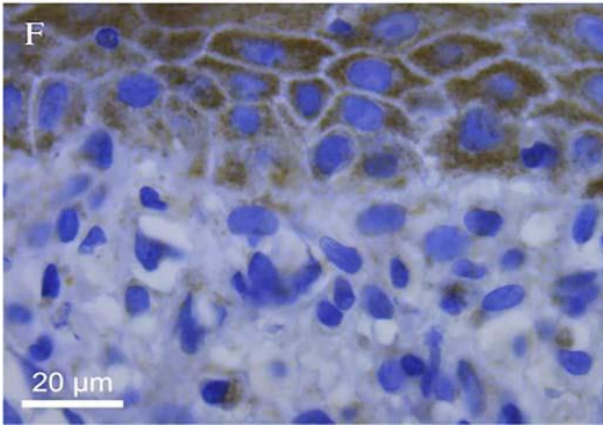
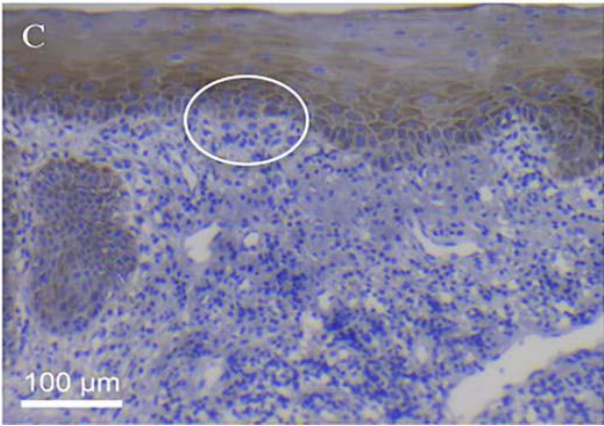
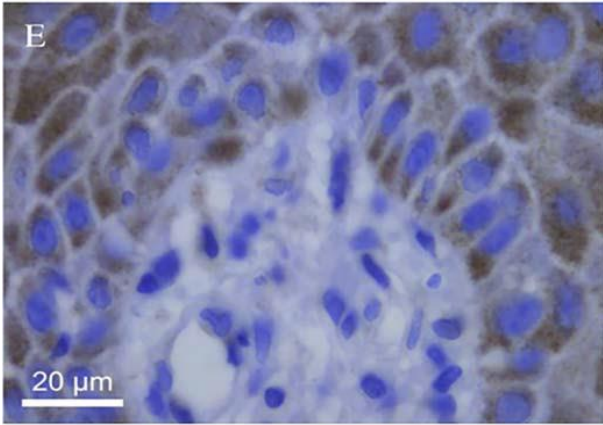
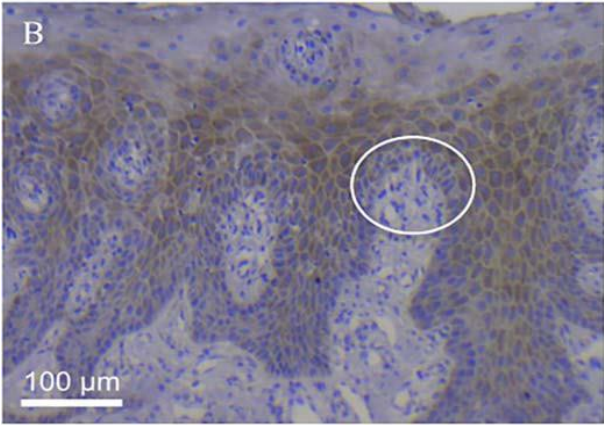
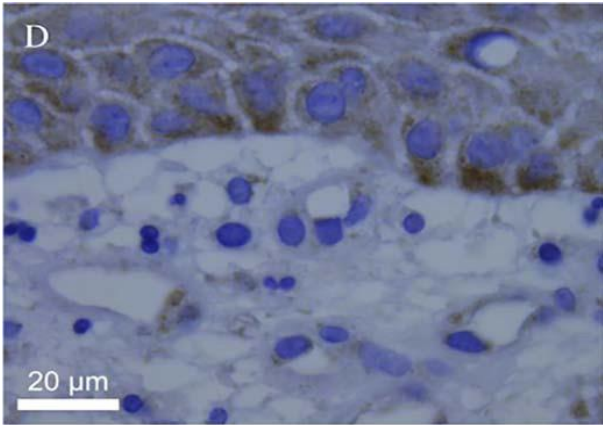
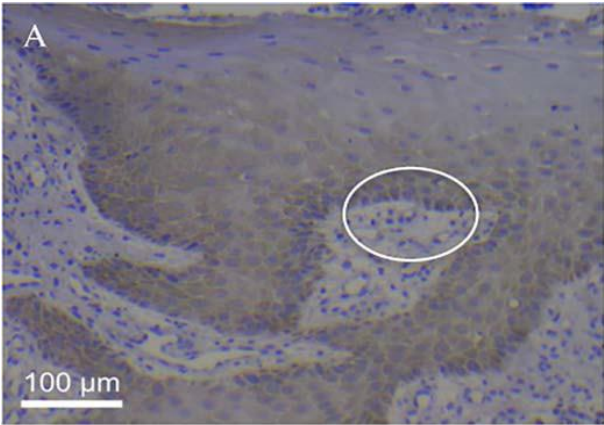


Figure.2



**Figure.3**



**Figure.4**

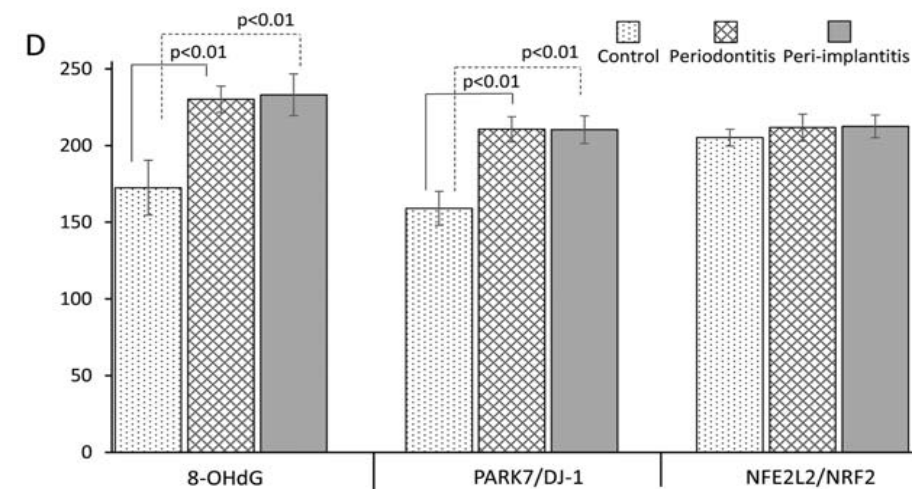
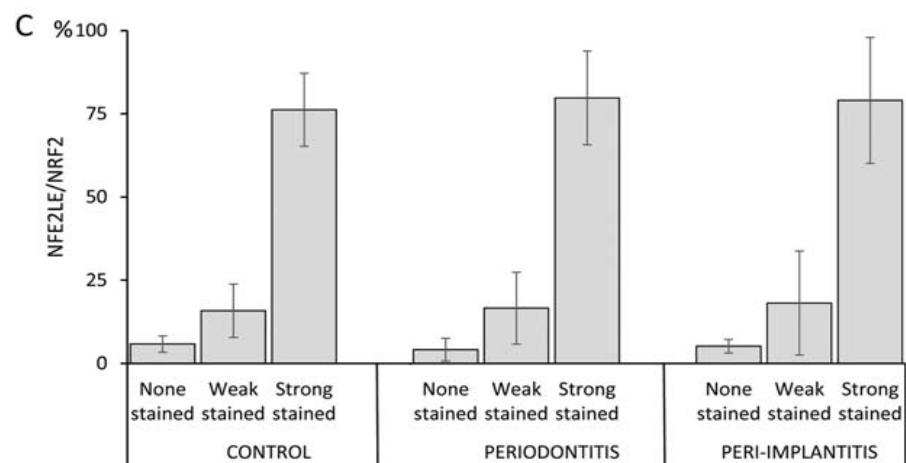
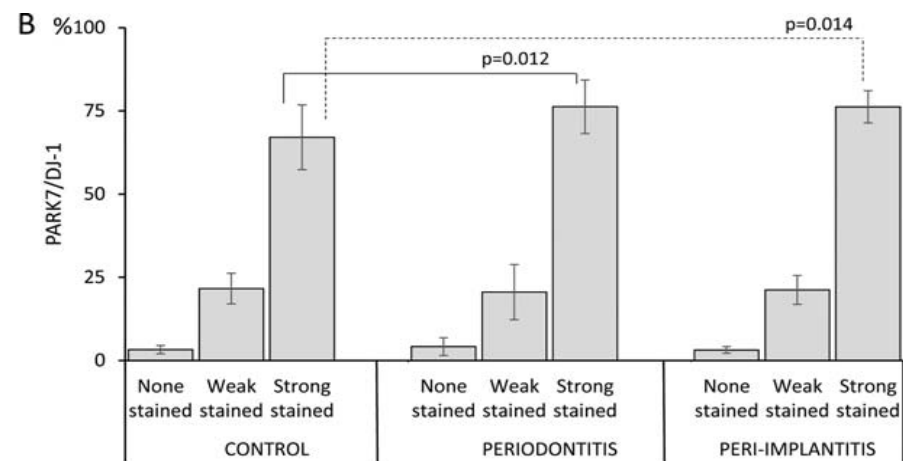
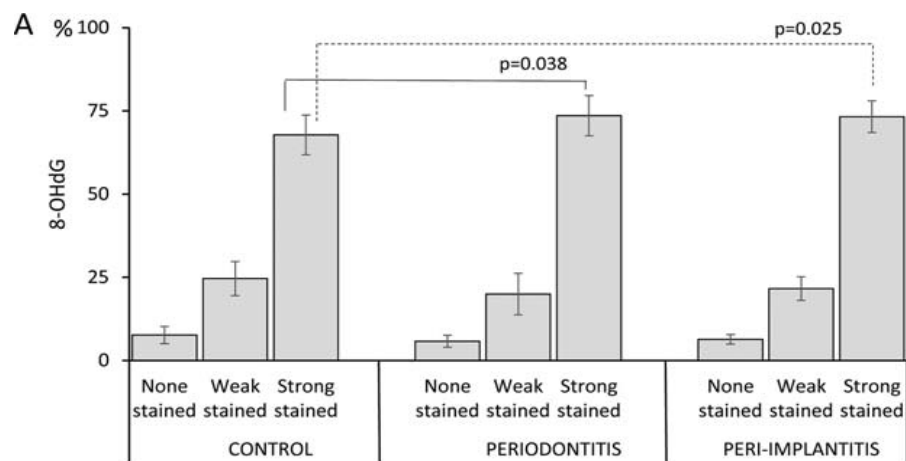
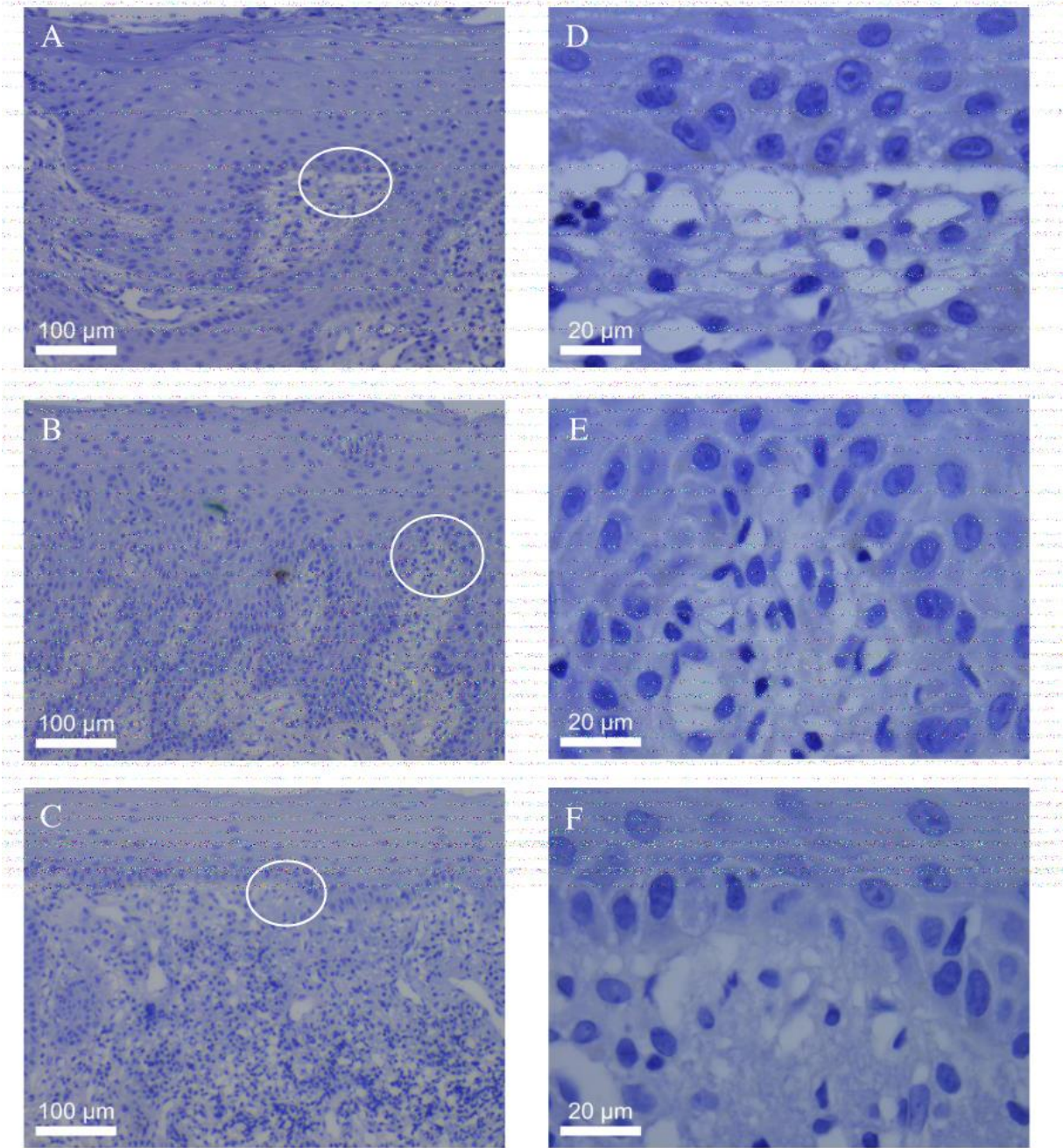
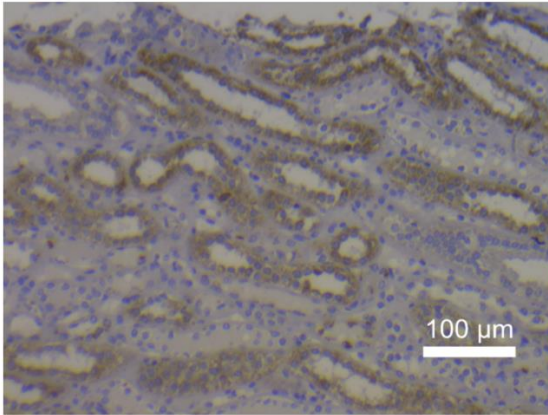


Figure.S1

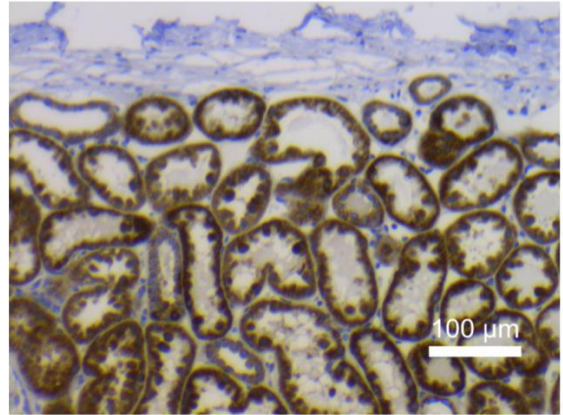


**Figure.S2**

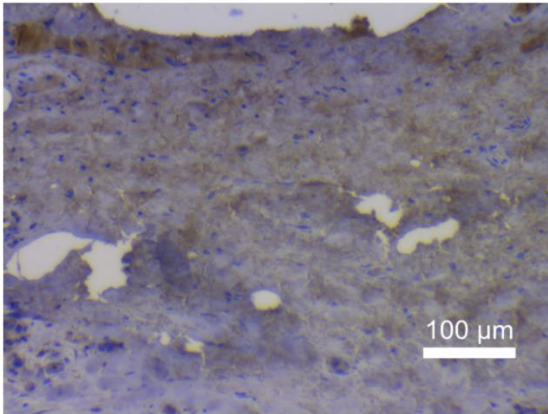
**KEAP1, Positive Control, Kidney**



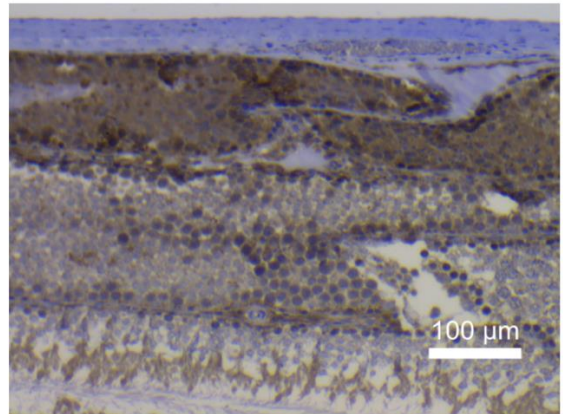
**NFE2L2/NRF2, Positive Control Kidney**



**8-OHdG, Positive Control, Lung**



**PARK7/DJ-1, Positive Control, Testis**



**Gingiva, Negative Control**

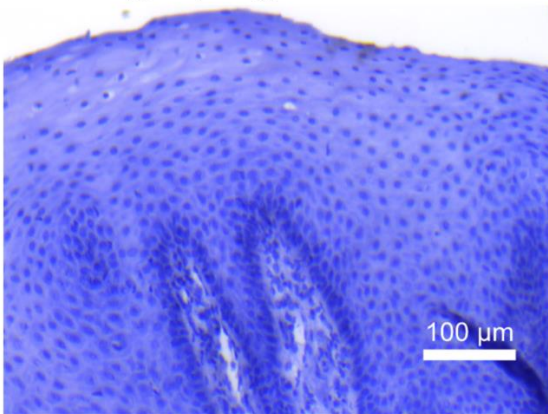


## Figure legends

### Figure.1

8-OHdG stainings with 20X (A-C) and 100X magnifications (D-F). The white circles indicate the area where the 100X images were taken. White arrows indicate the localization of the strongly stained epithelial cells, which were mainly located at the basal layer of the epithelium (A). In periodontitis (B) and in peri-implantitis (C) samples, 8-OHdG positive stainings were observed at all epithelial layers. 8-OHdG was detectable in the connective tissue control (D), periodontitis (E), and peri-implantitis (F) samples.

### Figure.2

PARK7/DJ-1 staining with 20X (A-C) and 100X magnifications (D-F). The white circles indicate the area where the 100X images were taken. In periodontally healthy controls, strongly stained epithelial cells were mainly located at the basal layer of the epithelium as pointed out with white arrows (A). In periodontitis (B) and in peri-implantitis (C) samples, PARK7/DJ-1 positive staining was found at all epithelial layers. PARK7/DJ-1 was evidently seen in the connective tissue of control (D), periodontitis (E), and peri-implantitis (F) samples.

### Figure.3

NFE2L2/NRF2 stainings with 20X (A-C) and 100X magnification (D-F). The white circles indicate the area where the 100X images were taken. NFE2L2/NRF2 was found at all epithelial layers in control (A), periodontitis (B) and peri-implantitis samples.

NFE2L2/ NRF2 was weakly stained in the connective tissue of control (D), periodontitis (E), and peri-implantitis (F) samples.

### Figure.4

The percentages of the stained cells in the study groups are illustrated as a bar graph. *P* values over the bars indicate a difference in the number of strongly stained cells (A-C) and the staining intensity of the images (D) between the study groups.

### **Figure.S1**

KEAP1 stainings with 20X (A,B,C) and 100X magnifications (D,E,F). The white circles indicate the area where the 100X images were taken.

### **Figure.S2**

The validities of the primary antibodies were tested on different human tissue samples. Negative control sections incubated with no primary antibody did not show any staining

### **Acknowledgments**

The authors are grateful to Mariia Valkama from the Institute of Dentistry, University of Turku, Finland, for her excellent technical assistance in immunohistochemical analyses. This study received Scandinavian Society of Periodontology 2017 Young researcher's award.

### **Funding**

This study was supported by the Turku University Foundation (Grant no: 12198, UKG) and by the Scientific and Technological Research Council of Turkey (Grant no: BIDEB 2219-1059B191600656, GK).

### **Conflict of Interest**

The authors declare that they have no conflict of interest.